



A NEW PLASMA METHOD OF SYNTHESIZING AEROSOL PARTICLES

G. Praburam* and J. Goree†

Department of Physics and Astronomy, The University of Iowa, Iowa City, IA 52242, U.S.A.

(First received 1 August 1995; and in final form 18 January 1996)

Abstract—A new experimental method of synthesizing aerosol particles is demonstrated. A non-thermal plasma is used to sputter a solid target by energetic ion impact. Sputtered atoms nucleate in the gas phase to form particles, which the plasma levitates particles during several hours of operation. Particle growth can take place at room temperature. The plasma is formed in a vacuum vessel by a pair of parallel electrodes that are powered with a radio-frequency high voltage. Scanning electron micrographs reveal the particle morphology. Particles initially grow with a spherical shape, and their size can be selected by terminating the discharge after they have grown to the desired diameter. By altering the plasma parameters such as gas pressure and voltage, and by allowing particles to grow for a longer period of time, they can coagulate into string-like or fractal-like conglomerates. Copyright © 1996 Elsevier Science Ltd

INTRODUCTION

Recently, it has been discovered that small particles can form under vacuum conditions in non-thermal gas discharge plasmas (Selwyn *et al.*, 1989; Ganguly *et al.*, 1993; Praburam and Goree 1994). To date, this type of particle production has received attention mainly from the microelectronic industry, where particulate growth during processing is a persistent and undesirable source of contamination. However, as a method of synthesizing particles, a gas discharge may be desirable for aerosol generation. The gas discharge allows controlled production of either isolated or coagulated particles, ranging in size from tens of nanometers to hundreds of microns. It can be compared to traditional condensation methods of generating aerosols, where particle sizes below 10 μm can be produced by Sinclair–La Mer generators, heated wires, exploding wires, high intensity arcs and plasma torches (Sinclair and La Mer, 1949; Phalen, 1972; Boffa and Pfender, 1973; Scheibel and Porstendofer, 1983; Ramamurthi and Leong, 1987).

Evaporation and condensation methods have certain limitations that can be remedied using our method. The particles' size distribution and their movement often cannot be controlled. They are not levitated for a long time in the region where they are formed. Also, a high temperature is required to evaporate a solid, and this is sometimes undesirable. The variety of materials that can be used is limited because the solid must evaporate at a reasonably low temperature in the presence of a vapor at a reasonably high pressure. Composite materials are difficult to synthesize, because the elemental constituents of alloys evaporate independently, at rates proportional to their respective vapor pressures. Another limitation is that particles generated by these methods grow as aggregates, which are often unwanted, for example due to optical properties that differ markedly from the those of isolated spheres. Because of these limitations of growth by evaporation, we report an alternative method—growth by sputtering in a gas discharge.

The gas discharge method employs a weakly ionized plasma, which is sustained typically by a radio-frequency high voltage. This produces energetic ions that bombard a solid target of a desired material. The material is sputtered at room temperature, yielding an atomic vapor consisting of sputtered atoms flying through the low-pressure gas that is present.

*Current address: Applied Materials, Santa Clara, CA, U.S.A.

†John.goree@uiowa.edu

These atoms collect on any particle that may have nucleated, making it grow by accretion. Particles are charged so that they are trapped and levitated by electric fields in the plasma. This levitation lasts for hours, and it keeps the particles in the region where they grow.

The plasma method of particle synthesis offers several advantages. It can produce an atomic vapor from a wider variety of materials than is possible with evaporation. This is because most solid materials, including composites, can be sputtered. Volatile elements such as oxygen can be incorporated into particles by adding them to the process gas. The process can be done not only at high temperatures as in evaporation sources, but also at room temperature as in our experiment or cryogenically, as in an experiment reported by Haaland (1995). Several discharge parameters are adjustable, giving control over the sputtering rate and therefore the particle growth rate and size distribution. Monodisperse size distributions can be produced for diameters of at least 150 nm, and the size can be selected, since it grows with time, simply by terminating the process. Coagulation is inhibited by the mutual electric repulsion of the particles. When particles exceed 150 nm diameter, the repulsion can be overcome just often enough to produce coagulated structures, including either string-like shapes or fractal conglomerates.

Here we report our phenomenological findings of how to synthesize various kinds of particle morphologies. For this demonstration, we used solid graphite targets which were sputtered with an argon plasma to grow carbon particles. After turning the discharge power off, particles fell to the lower electrode, allowing us to image them by scanning electron microscopy (SEM).

SYNTHESIS METHOD

Here we explain the principles involved in synthesizing particles. A partially ionized argon discharge is formed by applying a radio-frequency high voltage between two horizontal and parallel electrodes with a low gas pressure of typically 5×10^{-4} bar. The high voltage is responsible for sustaining the discharge by accelerating electrons to energies above the ionization threshold of the gas. The gas in the discharge is weakly ionized (fractional ionization $\sim 10^{-6}$) and non-thermal (electrons have a temperature of $\sim 2 \times 10^4$ K, ions and neutrals about 400 K). Argon is a suitable choice for the gas because Ar^+ ions provide a high sputtering yield, and it is inert and unlikely to be incorporated into the particles. If desired, other gases could be used. For example, oxygen could be used to synthesize silicates and other oxygen-bearing compounds, by sputtering an alloy target containing the other atomic elements that are required.

The plasma is concentrated in the region between the two electrodes. It is divided into two regions, a main plasma region that fills most of the inter-electrode spacing, and a sheath at the boundary between the plasma and the electrode, as sketched in Fig. 1. This sheath has a thickness of about 1 mm, and in it there is a strong localized electric field (~ 1 kV/cm) that points normal to the electrode surface. The sheath electric field confines the electrons in the plasma while expelling the ions. In the main plasma region there is a weaker electric field (~ 1 V/cm) which pushes ions away from the region where they are born by ionization. This field has both axial and a radial vector components; the axial component pushes ions toward the electrodes. The ion flow is collisional with the ambient neutral gas, and ions drift slowly out of the main plasma region due to the electric field and diffusion. Those that reach the sheath are accelerated rapidly toward the electrode surface, which they strike with an energy of several hundred electron volts. This sputters atoms of the electrode material, which fly away from the surface and thermalize with the ambient neutral gas after travelling a few millimeters. This is how the vapor of sputtered atoms is produced. They can nucleate to form a particle, or stick to a particle that already exists. Usually, the electrode is covered with a target made of a desired material, such as graphite, so that particles will be synthesized with the same composition. The process of particle growth by accretion of sputtered atoms is sketched in Fig. 1.

Particles are trapped in a localized region of the plasma by a combination of electrical, collisional, and gravitational forces. This trapping works as follows. For particles near the

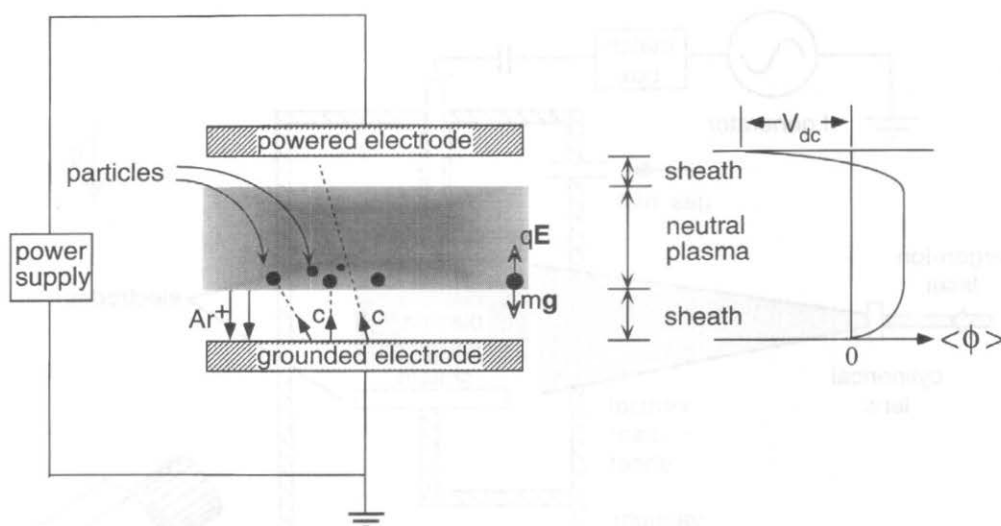


Fig. 1. Sketch of the particle synthesis process. Particles are electrically suspended in the plasma. Ions are extracted from the plasma and accelerated through the sheaths near the electrode surfaces. This acceleration leads to ions bombarding the surface and sputtering atoms from it. Atoms fly through the ambient gas and collect on grains so that they grow by accretion. Also shown is the electric potential profile between the electrodes, which provides the electrostatic levitation of negatively charged grains. (Reprinted from Praburam and Goree, 1995.)

lower electrode, the electrical force is upward, while the other forces are downward. The electrical force $F = QE$ is thus responsible for the levitation. The particle's charge Q develops because the particle collects electrons and ions. It is usually negative, due to the higher thermal velocity of the electrons. The plasma has an electric field E that is small in the central plasma region and strong in the sheath. This field develops naturally in any discharge to maintain electrical neutrality. The particles are levitated by the electric field at the height where the upward electric force balances the downward forces of gravity and collisional drag. Due to their smaller charge-to-mass ratio, larger particles are suspended at a lower height than small particles. All this pertains to the mechanism of levitating the particles in the vertical direction.

In the horizontal direction, particles are trapped by a gentle electric force that is directed toward the center of the plasma. This arises due to several effects, which together are often termed ambipolar diffusion. First, the electron and ion densities have spatial profiles that are peaked in the center. This is due to a balance between the source, which is ionization at a rate proportional to the electron density, and the loss, which is radial diffusion (plus a loss at the electrodes). The electron density n_e is related to the electric potential ϕ in the plasma by the Boltzmann relation, $n_e \propto \exp(e\phi/kT_e)$, or $\phi \propto \ln(n_e)$. Since the electron density is peaked in the center of the plasma and it has a radial gradient, so will the electric potential. The gradient $\nabla\phi$ is rather gentle due to the logarithmic dependence of the Boltzmann relation. The direction of the gradient is inward, radially. The electric force acting on a grain with charge Q is $-Q\nabla\phi$. Thus, this force has a gentle radial component. Its direction is radially inward, since the charge Q is negative. This acts to confine particles toward the plasma center, and prevent them from escaping in the radial direction.

APPARATUS

The experimental apparatus we used is sketched in Fig. 2. An aluminum vacuum vessel was used, and it is cylindrical, with an inner diameter of 32.4 cm and a height of 31.6 cm. For making optical measurements, it is anodized black to reduce scattered light and fitted with Pyrex windows

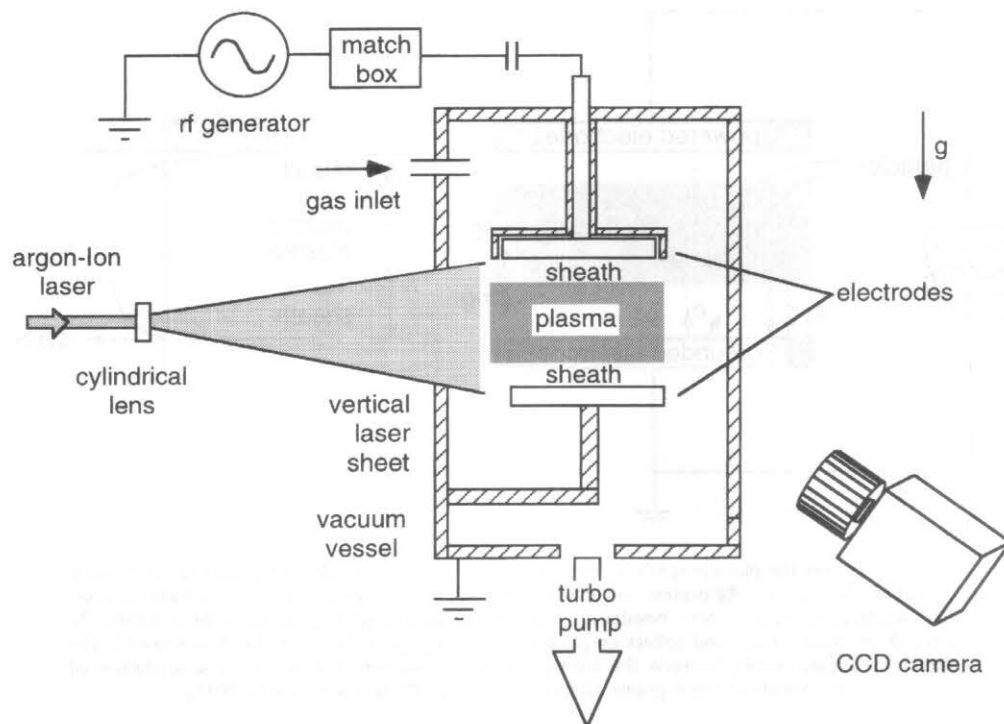


Fig. 2. Schematic of apparatus. The graphite electrodes are removable, for performing scanning electron microscopy on the particles that collect on them. The upper electrode is powered and water cooled, and it is fitted with a ground shield. The lower electrode is grounded. Particles suspended in the plasma are illuminated by a vertical sheet of argon-ion laser light and imaged by a monochrome video camera.

The electrodes are 6.2 cm diameter, and each is covered by a disk-shaped graphite target. The electrode plates are parallel, with a separation of 2 cm. The upper electrode is water-cooled, since most of the ≈ 100 W of power is ultimately deposited there. The targets were clamped to a stainless steel base by a circular ring, which was recessed 0.5 mm below the surface of the graphite plate, since tests reported elsewhere revealed this yields a larger collection of particles after the plasma is extinguished (Praburam and Goree, 1994).

The upper electrode was powered by a 13.6 MHz sinusoidal signal supplied by a function generator driving a broadband amplifier (Amplifier Research 200A15). The impedances of the amplifier output and the discharge were matched using a pi-type network followed by a $0.019 \mu\text{F}$ coupling capacitor. The coupling capacitor allows the powered electrode to float electrically to a large negative D.C. "self-bias," (Lieberman and Lichtenberg, 1994) which was measured as -470 V in our experiment, for an argon pressure of 5.5×10^{-4} bar and an R.F. power of 110 W. This self-bias is responsible for much of the ion acceleration that causes the sputtering. The upper electrode assembly is surrounded by a ground shield to minimize discharge formation along the sides of the electrode assembly. The bottom electrode and the chamber walls are grounded.

Argon gas flowed through the vacuum vessel during operation. It was admitted through an inlet on the side wall of the chamber and evacuated by a turbo-molecular pump backed by a mechanical pump. The gas flow rate was typically 140 sccm. The gas inflow rate was regulated to maintain a constant gas pressure. At 5.5×10^{-4} bar, this pressure was six orders of magnitude higher than the vacuum vessel's base pressure (due to water and nitrogen). Because of this and the relatively oil-free nature of turbo-molecular pumps, we believe that gas-phase contaminants were not incorporated into the particles during their growth to any meaningful extent.

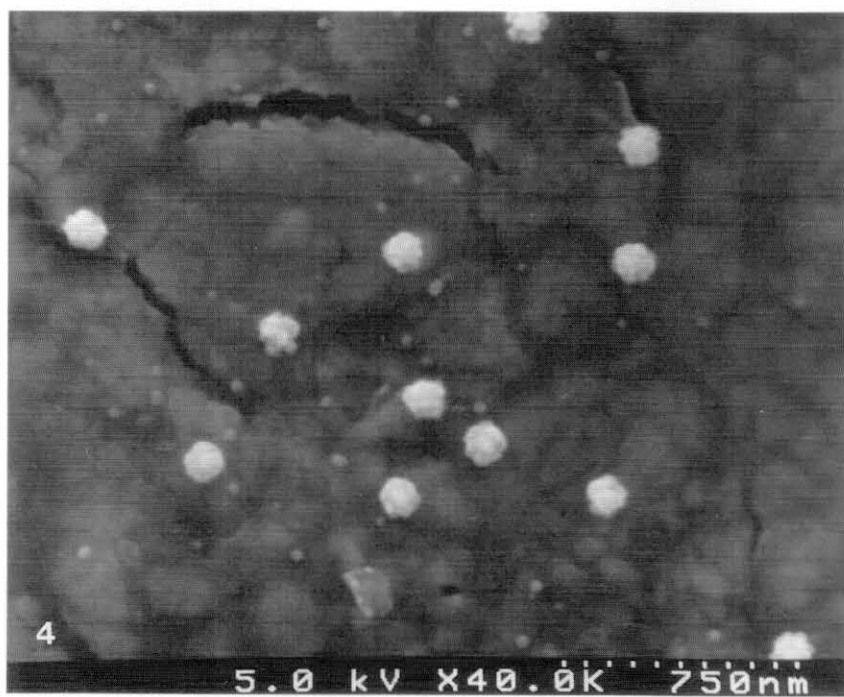
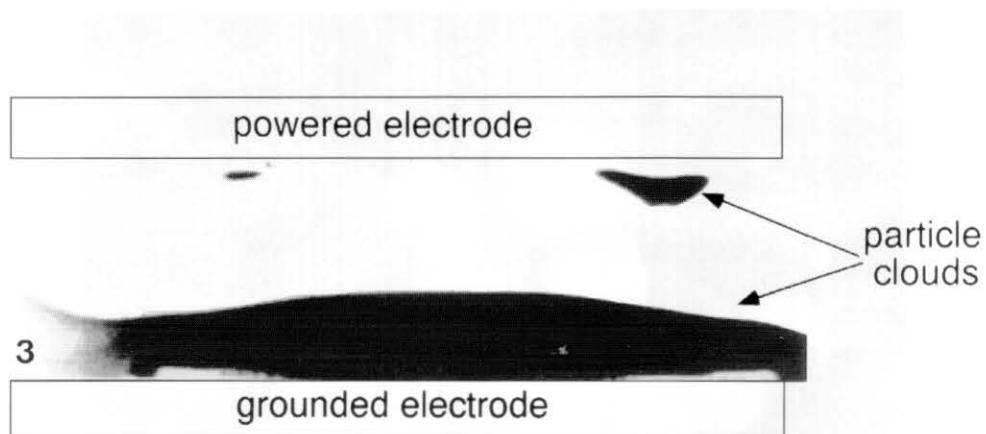


Fig. 3. Video image of the particulate cloud after 6 min of discharge operation. In this experiment the particulates, too small to be imaged individually, are seen as a cloud. As the camera viewed the scattered light at 45° the dust cloud appears compressed by $1/\sqrt{2}$ in the horizontal direction.

Fig. 4. SEM images of carbon grains collected after 10 min of plasma exposure. The discharge was operated at 5.5×10^{-4} bar argon pressure and 110 W rf power. The particles have a uniform 100–150 nm size distribution and are uncoagulated. The beam voltage of 10 keV used in the SEM for this and some other figures altered the surface texture of the grains, smoothing them so that they do not resemble a cauliflower. Figures 5–7 continue this time sequence, and all were prepared using the same discharge conditions (but varying magnifications in the micrographs).

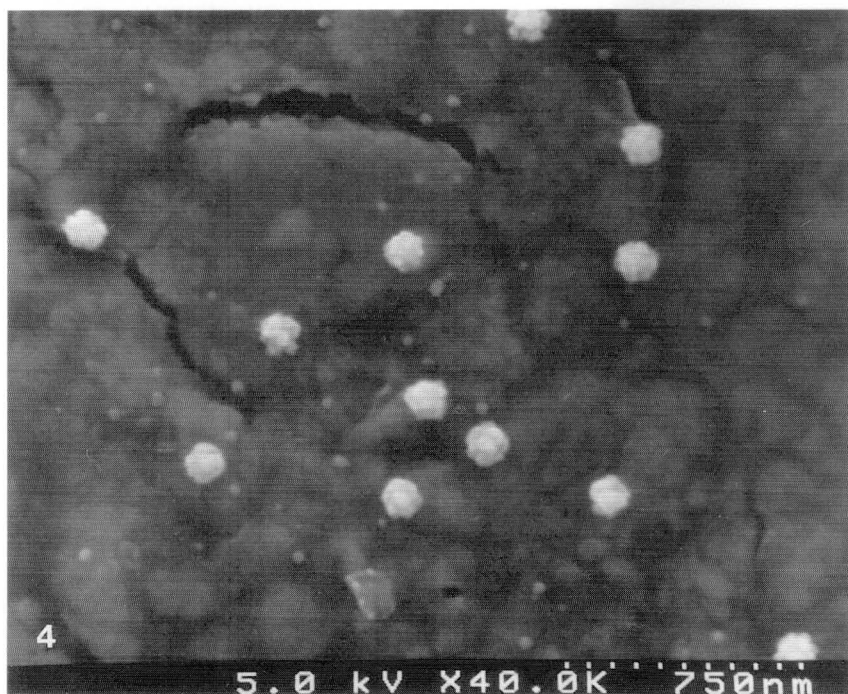
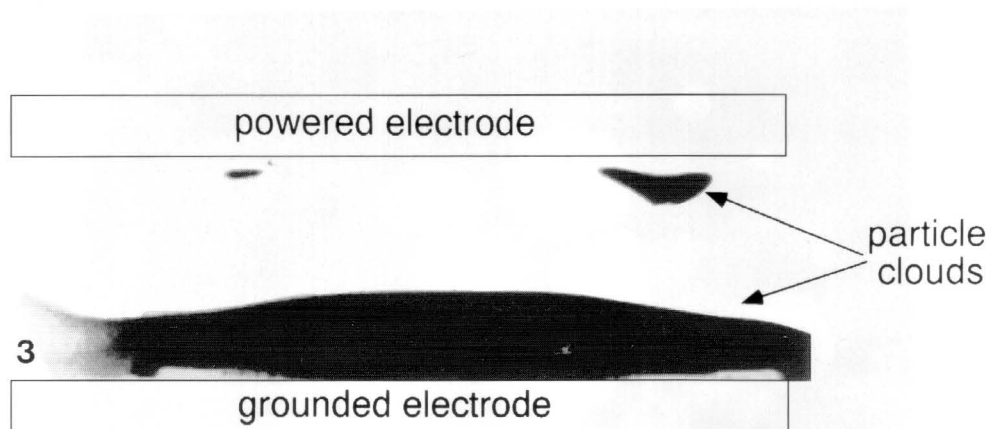


Fig. 3. Video image of the particulate cloud after 6 min of discharge operation. In this experiment the particulates, too small to be imaged individually, are seen as a cloud. As the camera viewed the scattered light at 45° the dust cloud appears compressed by $1/\sqrt{2}$ in the horizontal direction.

Fig. 4. SEM images of carbon grains collected after 10 min of plasma exposure. The discharge was operated at 5.5×10^{-4} bar argon pressure and 110 W rf power. The particles have a uniform 100–150 nm size distribution and are uncoagulated. The beam voltage of 10 keV used in the SEM for this and some other figures altered the surface texture of the grains, smoothing them so that they do not resemble a cauliflower. Figures 5–7 continue this time sequence, and all were prepared using the same discharge conditions (but varying magnifications in the micrographs).



Fig. 5. Carbon grain collected after 20 min. Note the particles that appear to have stuck together.

Fig. 6. Carbon grains collected after 40 min. The particles have a wide size distribution. Note the coagulated structure of larger grains, and the spongy structure of smaller nanometer scale grains, which are too small to analyse using the SEM.

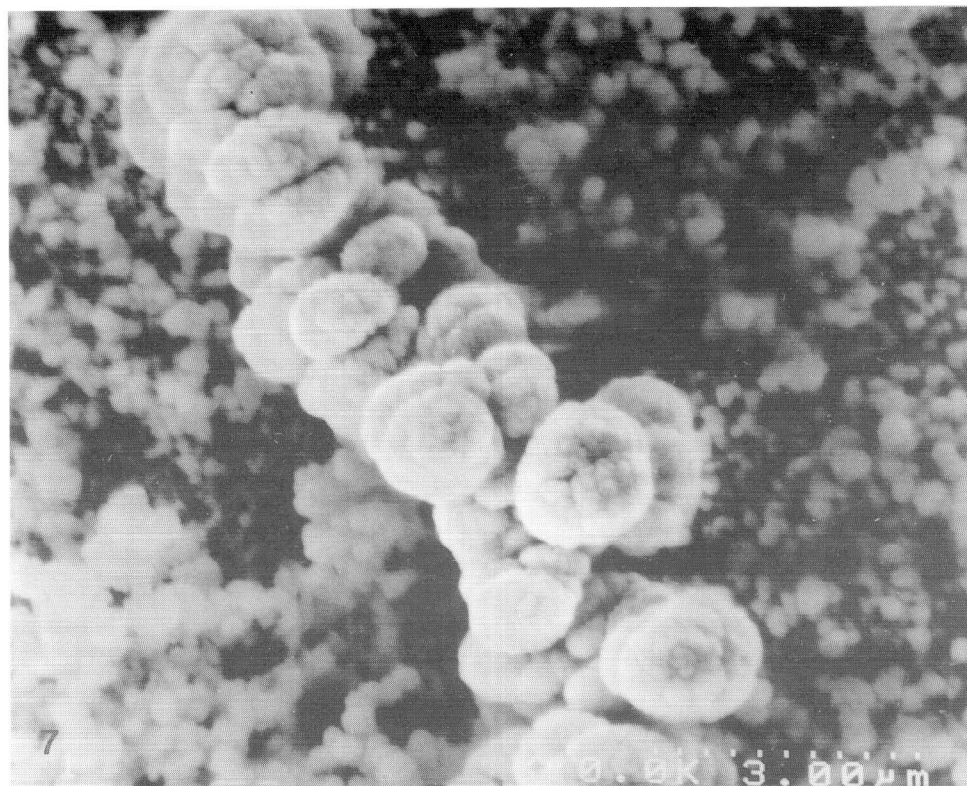


Fig. 7. Carbon grains collected after 420 min. The spheroids have a cauliflower-like surface structure. Particles of $1 \mu\text{m}$ size have stuck together, forming a coagulated string. The flatness of the spheroids indicates further growth by accretion following coagulation.

Fig. 8. SEM images of carbon particles with fractal structure, collected in the experiment that yielded Fig. 6.

We used laser light scattering to monitor the particle growth *in situ*. An argon-ion laser beam ($\lambda = 488$ nm) was operated at a power of 500 mW and directed through a cylindrical lens to form a vertical sheet of light, as shown in Fig. 2. Video images of the particle cloud were produced using a monochrome camera equipped with a band pass interference filter to block the plasma glow. It viewed the scattered light at 45° ; thus, the dust cloud appears compressed by $1/\sqrt{2}$ in the horizontal direction. Images were digitized by a frame grabber.

After turning the plasma off, many particles fell onto the lower electrode. We then transferred the electrode from the vacuum chamber into a scanning electron microscope (SEM), without disturbing the particles. This allowed us to characterize the size and morphology of the particles. Usually, the SEM was operated at ≈ 4 keV, but sometimes it was necessary to use a higher beam energy of 10 keV, which caused a slight melting of the particle surface that is detectable in our images.

RESULTS

Particle growth

We carried out several experiments to observe the particle growth process. Within minutes of turning on the discharge, particles grew to a detectable size. They were levitated near the plasma-sheath boundary. This was revealed by the light scattering monitor. Figure 3 shows a video image of the particulate cloud 3 min after the discharge was started. The cloud evolved over time, with a complicated cycle of growth and collapse that is described in detail elsewhere (Praburam and Goree, 1994; Praburam and Goree, 1995b).

During the first few minutes of operation, particles grew as individual spheres with a diameter that increased with time. This is attributed to growth by accretion, in which an atom or molecule strikes a particle and sticks to it. During this stage, electrostatic repulsion prevents particles from coagulating.

At a later stage, under certain plasma parameters, particles can collide to form conglomerates with fractal or coagulated strings. Fractal particles were attained by operating with an argon pressure $> 5.5 \times 10^{-4}$ bar. By increasing the R.F. power to > 110 W, coagulated strings were formed. The growth mechanism is apparently sensitive to a slight change in R.F. power.

Individual particles

Uncoagulated spheroidal particles were produced during the first 10 min of plasma exposure. These have a roughened surface that resembles a cauliflower, as shown in Fig. 4. This shape is not peculiar to our experiment. Other investigators using similar R.F. discharges and of slightly different design have reported growing similar cauliflower-shaped particles (Selwyn *et al.*, 1989; Ganguly *et al.*, 1993). The temperature of the particle's surface during growth by accretion plays a large role in determining the surface roughness (Praburam and Goree, 1995a). Another experimenter (Haaland, 1995) found that the bumps on the surface have a more angular or crystalline appearance when the apparatus is cooled to liquid nitrogen temperature.

The diameter of the spheroidal particles after 10 min of plasma exposure was (154 ± 10) nm. The ± 10 nm diameter range is the one-sigma level of the size dispersion. After 20 min, the diameter of the spheroids had doubled, indicating a linear growth rate of about 15 nm/min.

The growth rate due to accretion can be calculated as follows. The flux Γ_c of sputtered carbon atoms is related to the incident ion flux Γ_i by $\Gamma_c = Y\Gamma_i$, where Y is a material parameter called the sputtering yield. The ion flux is given by the ion current density J_i , so that $\Gamma_i = J_i/e$. The sputtered atoms are essentially isotropic after passing from the target through a few millimeters of the neutral gas (Praburam and Goree, 1995a). Thus, they strike a suspended spherical particle equally on all sides, so that it grows in volume V at a rate

$dV/dt = \Gamma_c 4\pi a^2 T^3$, where a is the particle radius and T is the thickness of one monolayer of adsorbed atoms on the surface of the grain. Equating this with $dV/dt = 4\pi a^2 da/dt$ yields

$$da/dt = YJ_i T^3/e. \quad (1)$$

Note that equation (1) gives a constant growth rate, independent of the particle size. The ion current to the electrode J_i can be estimated, within a factor of two, by dividing the radio-frequency (RF) power by the DC self-bias and the electrode area. This is equivalent to approximating that all of the RF power is used in accelerating ions through the DC self-bias. In our experiment this yields $J_i = 7.6 \text{ A/m}^2$. The sputtering yield for argon ions with an energy of a few hundred electron volts incident on graphite is approximately $Y = 0.1$, and the atomic diameter of carbon is $T = 0.136 \text{ nm}$. Using this in equation (1) yields a particle diameter growth rate of $2 da/dt = 14 \text{ nm/min}^{-1}$, which agrees well with the experimentally determined rate of 15 nm/min^{-1} during the first 20 min of operation. This agreement lends confidence to the idea that in our experiment the spheres grow by accretion of neutral sputtered atoms. In a slightly different experiment, however, Haaland (1995) found better agreement by assuming that the carbon atoms are ionized (by electron impact) before they are collected by the negatively charged sphere. That experiment differed from ours in the use of a different radio frequency (100 kHz instead of 13 MHz) and a different gas (He instead of Ar).

Coagulated particles

In a coagulation process, particles collide with one another and stick, forming a shape that is non-spherical and often fractal (Russel *et al.*, 1989). In a vacuum, the sticking is due to van der Waals attraction (Weidenschilling, 1980). It can happen only if the collision velocity is below a critical speed so that the particles do not bounce apart. The critical speed depends on the particle size and the elastic properties and surface energy of the material (Chokshi *et al.*, 1993; Dahneke, 1971). The strength of attraction depends on the surface roughness and geometry of the contact area of the particles.

Coagulated particles were synthesized in our experiment. This happened when the apparatus was operated with an argon pressure of 5.5×10^{-4} bar and an RF power of 110 W. The temporal development of the particle growth is shown in the time series of SEM micrographs shown in Figs 4–7. The particles were grown during runs of 10, 20, 40 and 420 min, all with identical conditions. These micrographs show that as the exposure time is increased, particles grow larger in diameter, and they are more likely to be coagulated. The number of spheroids per coagulated particle also increases with time. These results are reviewed below.

After 10 min (Fig. 4) particles were fairly monodisperse (150 nm) and were not yet coagulated. At this point in their growth they had a spheroidal shape resembling a raspberry. The bumps on the surface grow over time, so that the spheroid eventually acquires a cauliflower appearance. After 20 min (Fig. 5) spheroids were larger, again with a narrow size distribution (300 nm). Many were coagulated, with a maximum of 10 particles in each conglomerate. (The spheroid's morphology in Fig. 5 looks different from a cauliflower due to a slight melting that occurred in the SEM when a beam voltage of 10 keV was used.) After 40 min (Fig. 6) particles had a wide distribution of sizes (a few nanometers to 500 nm) and were coagulated. We presume that the smaller particles are younger than the larger ones. The largest feature in Fig. 6 is a coagulated structure, where 400–500 nm spheroids are stuck together to form a cluster. Compared to the coagulated structure shown in Fig. 6 (particles grown for 20 min), this one is larger, with more particles stuck together. After 420 min (Fig. 7), we observed a few large string-shaped clusters of micron-size particles. The particles in the coagulated structure are non-spherical, with a flattened shape that is probably due to growth by accretion following the coagulation (Praburam and Goree, 1995a). Note the cauliflower-like appearance of the spheroids in this particle.

To validate our coagulation results, it is necessary to verify that these particles coagulated when they were suspended in the gas phase. We do this by ruling out all the other

possibilities. We can exclude the possibility of coagulating during *ex situ* handling after the plasma was turned off, because we avoided any handling. The particles deposited on the electrode were left undisturbed, and the entire electrode was transferred into the SEM. Another possibility is that the particles landed upon one another and formed a cluster on the electrode. This can be excluded, since we found that the number of spheroids in a coagulated structure increases with exposure time, which is unrelated to the process of falling when the plasma is extinguished.

Coagulation of electrically charged particles requires a large inter-particle velocity to overcome the repulsive potential. This velocity must be far higher than the thermal velocity at the neutral gas temperature. Thus, super-thermal particles are thought to be responsible for coagulation in our experiments. Measurements of particles large enough to image individually indicate that a fraction have a super-thermal velocity, which is consistent with our coagulation observations (Praburam and Goree, 1995a).

Fractal particles

Large spongy structures composed of nanometer-size particles were observed under some plasma conditions. Figure 8 shows a typical void-filled spongy structure. The SEM revealed that this sponge covers not just the area shown in the image, but the entire electrode surface. Larger spheroids happen to rest upon this structure. The spongy structure apparently consists of individual particles, too small to image with the SEM, separated with many voids. These structures were often found when the discharge was operated at pressures $> 5.5 \times 10^{-4}$ bar, the same conditions that also led to coagulation of larger spheroids, as described above.

While we believe the growth mechanism during the early stage of isolated spheroid growth is well understood, we cannot explain the growth mechanics during the later stage of producing the coagulated and fractal particles. We do not know why a certain RF power or gas pressure leads to certain particle morphology. The experimenter must adopt a phenomenological approach to synthesize a desired shape. The operating parameters that lead to a certain morphology are likely to vary from one apparatus to another.

SUMMARY

We have demonstrated how particulates can be synthesized in an electrostatic suspension. A low-pressure plasma powered by a radio-frequency high voltage is used to sputter a target. This produces a flux of atoms, which promotes particle growth by accretion. The particles are levitated and suspended in the plasma during several hours of plasma operation. They grow at room temperature by accretion and coagulation. In our demonstration, we grew carbon particles. The particles we collected were usually spherical, with a size that increased with exposure time. They had a cauliflower-like surface. Under some conditions, our method yielded coagulated particles composed of spherical cauliflowers pressed together in string-shaped masses or fractal particles.

Acknowledgement—This work was supported by NASA NAGW-3126, NASA NAG8-292, and NSF ECS-92-15882.

REFERENCES

- Boffa, C. V. and Pfender, E. (1973) Controlled generation of aerosols in the sub-micron range. *J. Aerosol Sci.* **4**, 103.
Chokshi, A., Tielens, A. G. G. M. and Hollenbach, D. (1993) Dust coagulation. *Appl. Phys. J.* **407**, 806.
Dahneke, B. (1971) The capture of aerosol particles by surfaces. *J. Colloid Interface Sci.* **37**, 342.
Ganguly, B., Garscadden, A., Williams, J. and Haaland, P. (1993) Growth and morphology of carbon grains. *J. Vac. Sci. Technol. A* **11**, 1119.
Haaland, P. (1995) In *Proc. 6th Workshop on the Physics of Dusty Plasmas*. University of California, San Diego, March 1995 (Edited by P. K. Shukla and A. Mendis), World Scientific Press, Singapore (in press).
Lieberman, M. A. and Lichtenberg, A. J. (1994) *Principles of Plasma Discharges and Materials Processing*. Wiley,

- Phalen, R. F. (1972) Evaluation of an exploded-wire aerosol generator for use in inhalation studies. *J. Aerosol Sci.* **3**, 395.
- Praburam, G. and Goree, J. (1994) Observations of particle layers levitated in an rf sputtering plasma. *J. Vac. Sci. Technol. A* **12**, 3137.
- Praburam, G. and Goree, J. (1995a) Cosmic dust synthesis by accretion and coagulation. *Appl. J.* **441**, 830.
- Praburam, G. and Goree, J. (1995b) Evolution of a particulate cloud in an RF plasma. *IEEE Trans. Plasma Sci.* (submitted).
- Ramamurthi, M. and Leong, K. H. (1987) Generation of monodisperse metallic, metal oxide and carbon aerosols. *J. Aerosol Sci.* **18**, 175.
- Russel, W. B., Saville, D. A. and Schowalter, W. R. (1989) *Colloidal Dispersion*. Cambridge Press, Cambridge.
- Scheibel, H. G. and Portstendorfer, J. (1983) Generation of monodisperse Ag- and NaCl-aerosols with particle diameters between 2 and 300 nm. *J. Aerosol Sci.* **14**, 113.
- Selwyn, G. S., Singh, J. and Bennett, R. S. (1989) *In situ* laser diagnostic studies of plasma-generated particulate contamination. *J. Vac. Sci. Technol. A* **7**, 2758.
- Sinclair, D. and La Mer, V. K. (1949) Light scattering as a measure of particle size in aerosols. *Chem. Rev.* **44**, 245.
- Weidenschilling, S. J. (1980) Dust to planetesimals: Settling and coagulation in the solar nebula. *ICARUS* **44**, 172.